Int J Clin Exp Pathol 2015;8(12):16111-16116
www.ijcep.com /ISSN:1936-2625/IJCEP0014889

Original Article

CT features and pathologic characteristics of IgG4-related systemic disease of submandibular gland

Zhiwei Wang[1*], Ruie Feng[2*], Yu Chen[1], Miao Duan[1], Man Wang[1], Zhengyu Jin[1], Zoran Rumboldt[3], Zhuhua Zhang[1]

Departments of [1]Radiology, [2]Pathology, Peking Union Medical College Hospital, Beijing, 100730, China; [3]Medical University of South Carolina, Charleston, SC, USA. [*]Equal contributors.

Received May 29, 2015; Accepted Novembe 19, 2015; Epub December 1, 2015; Published December 15, 2015

Abstract: The submandibular gland is one of the most frequently affected salivary gland in IgG4-related systemic disease, usually demonstrate homogeneous attenuation on CT imaging as reported, but without much pathological comparison of many cases. This article is to investigate and analyze the typical CT findings and pathologic characteristics of IgG4-related systemic disease (IgG4-RSD) of submandibular gland. A retrospective analysis of the preoperative CT findings in patients with IgG4-RSD of submandibular glands who underwent surgical resection between January 2010 and February 2014 was performed. Twenty patients (16 women) were identified, with a mean age of 58.1±10.2 years. All patients presented with painless submandibular gland swelling. Diffuse gland enlargement, with clear margins and homogeneous density, was found on non-enhanced CT scans in all cases. There were no calcifications or stones within the involved glands. Based on contrast-enhanced CT appearance the patients could be divided into two groups: 11 cases showed homogeneous gland enhancement; and multiple hyperenhancing foci, with a crazy-paving pattern, were detected in 9 cases, which were in consistent with the pathologic findings. The maximum submandibular gland diameter on transverse images was significantly larger (P=0.008) in patients with crazy-paving appearance (32±4 mm) compared to patients with homogeneous enhancement (28±3 mm). It is concluded that the submandibular glands with IgG4-RSD can be characterized by either homogenous appearance or crazy-paving pattern on contrast-enhanced CT imaging.

Keywords: Computed tomography, IgG4-related systemic disease, submandibular gland

Introduction

IgG4-related systemic disease (IgG4-RSD) has been recently characterized by a dense lymphoplasmacytic infiltrate rich in IgG4-positive plasma cells, storiform-type fibrosis and obliterative phlebitis, and elevated levels of serum IgG4 [1, 2]. Since its first description as autoimmune pancreatitis (AIP), many extrapancreatic manifestations have been reported, even in the absence of pancreatitis. The head and neck region is the second most commonly affected site, after the pancreatobiliary system [3-5]. The radiological features and pathologic characteristics of IgG4-related lesions of pancreatic, renal, and pulmonary lesions have been well documented [6, 7]. In the head and neck, most previous reports have focused on magnetic resonance imaging (MRI) findings and the salivary gland features have not been specifically described [5, 8-12]. Our goal was to analyze the computed tomography (CT) manifestation and pathological features of affected submandibular glands, with the hypothesis that IgG4-RSD exhibits characteristic imaging findings.

Material and methods

Subjects

This study was approved by the Institutional Review Board. Between January 2010 and February 2014, 20 patients with histopathologically confirmed IgG4-RSD in the submandibular glands were identified at our institution and included in this study. The clinical data were obtained from the medical records. All patients underwent contrast enhanced CT scan at initial presentation.

Table 1. Patient demographics and CT features

Patient	Sex	Age	IgG4 level before surgery (80-1400 mg/L)	Previous unilateral submandibular gland excision	Homogeneous or heterogeneous enhancement	Largest axial diameter of the gland (cm)	Other IgG4-related lesions during follow-up
1	F	60	13900	+	homogeneous	2.81	lacrimal glands, pancreas, mediastinal and abdominal lymphadenopathy
2	M	55		+	heterogeneous	3.38	pancreas
3	F	62		-	heterogeneous	3.07	lacrimal glands
4	M	47		-	homogeneous	2.91	
5	M	72		-	heterogeneous	3.27	lung
6	F	79		+	homogeneous	3.33	mediastinal and abdominal lymphadenopathy
7	F	47		-	heterogeneous	2.74	
8	F	48	10100	-	homogeneous	2.82	lacrimal glands
9	F	79	8210	+	homogeneous	2.41	lung, pancreas, liver and kidneys
10	F	56		-	homogeneous	2.56	
11	F	53	9990	-	heterogeneous	3.42	pancreas and kidneys
12	F	58		-	heterogeneous	3.56	parotid gland
13	F	58		-	homogeneous	2.71	
14	F	53		-	heterogeneous	2.97	lacrimal glands and parotid gland
15	F	59		-	homogeneous	2.41	
16	F	46		+	heterogeneous	3.41	
17	F	56	3040	-	homogeneous	3.64	lacrimal glands
18	M	49		-	homogeneous	2.35	
19	F	64		-	heterogeneous	3.33	
20	F	58		-	homogeneous	2.39	lacrimal glands

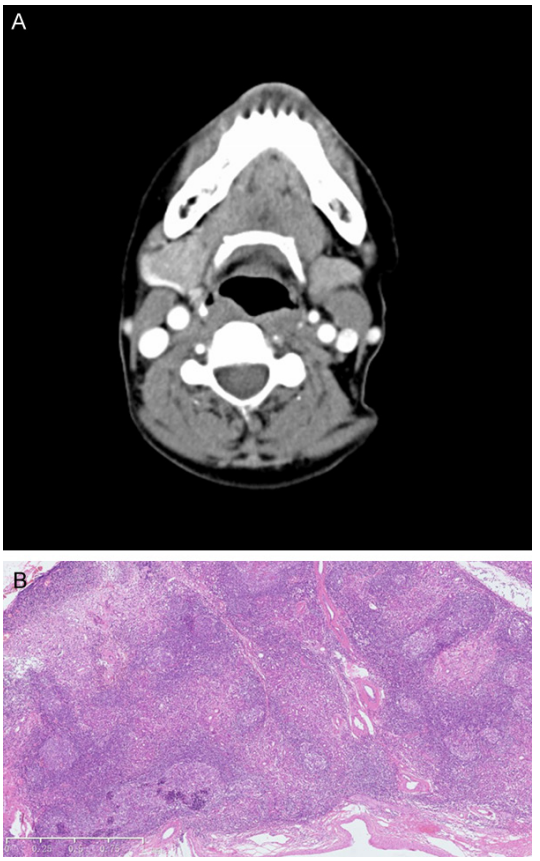

Figure 1. A. Contrast-enhanced axial CT image in patient 15. The right submandibular gland is enlarged, showing homogeneous attenuation. B. Histopathologic examination of the right submandibular gland reveals destruction of the normal structure of the gland with marked infiltration of lymphocytes and plasma cells.

CT scanning

All neck CT studies were performed with helical CT scanners (Somatom Definition Flash or Sensation 64, Siemens Healthcare, Forchheim, Germany). A biphasic CT protocol was performed in every patient and consisted of an unenhanced and an enhanced acquisition. A total of 90 mL of iopamidol (Ultravist 300 mgI/ml, Bayer Schering) was administered into an antecubital vein at a rate of 2.5 mL/sec by using a power injector. The images were then obtained with a scanning delay of 25 seconds. Contiguous transverse images were reconstructed at 4-mm intervals.

CT evaluation

Two radiologists (with 6 and 16 years of head and neck imaging experience) retrospectively reviewed the CT scans in one image interpretation section. The submandibular and parotid glands were specifically evaluated and largest diameter was measured on transverse images. Decisions regarding the CT features were determined in consensus, with particular attention to the location and number of lesions, internal architecture, enhancement patterns, presence of calcification, vascular occlusion or compression, and cervical lymph nodes. On post-contrast CT images, the enhancement pattern of the lesions was categorized as either homogeneous or heterogeneous, and specific patterns were described. Lymph nodes were considered enlarged if their maximal short-axis diameters were greater than 1 cm on axial images. The groups with different imaging features were compared. The CT characteristics of the submandibular glands were also compared to the histological features.

Histological diagnosis

In all patients, histological diagnosis of IgG4-RSD was established following surgical resection. Histopathology was reviewed by a dedicated head and neck pathologist with 25 years of experience.

Statistical analyses

Statistical analyses were performed using statistical software (SPSS, version 13.0, Chicago, IL, USA). Fisher's exact test was used for comparison between the two groups. *P* values of 0.05 and below were considered statistically significant.

Results

The group of 20 patients included 4 men and 16 women, with a mean age of 58.1±10.2 years. All patients presented with painless en larged submandibular gland, with the duration of symptoms ranging from 3 months to 5 years. Serum IgG4 was tested in five patients and they all had increased IgG4 levels. The clinical, laboratory, and imaging features are listed in **Table 1**. Five of the patients had previous unilateral submandibular gland excision, 1 to 4 years prior to this presentation.

CT showed diffuse submandibular gland enlargement, with clear margins and homogeneous density in non-enhanced images. Among the 15 cases without prior unilateral gland resection, symmetrical bilateral enlargement of the submandibular glands was present in 13,

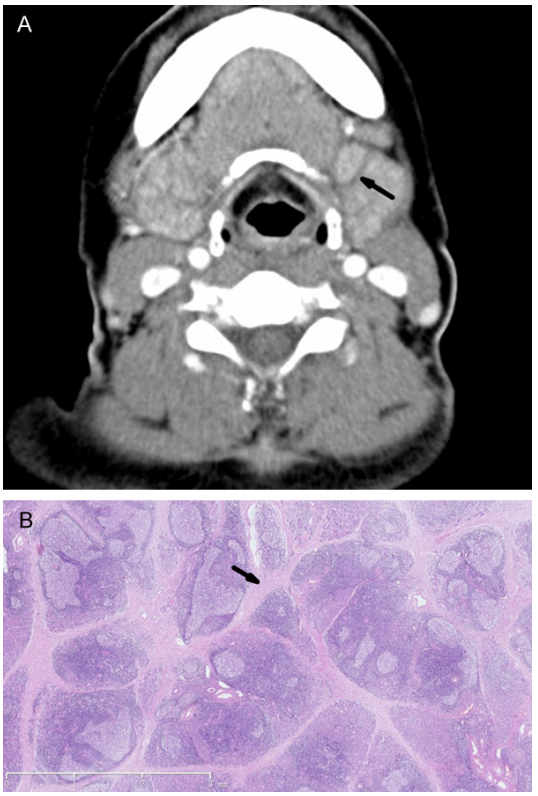

Figure 2. A. Contrast-enhanced CT axial images of the submandibular gland in patient 16. Note the glands are bilaterally enlarged, showing heterogeneous attenuation with a crazy-paving pattern. B. Histopathologic examination of the submandibular gland shows destruction of the normal gland structure with thick fibrous bands (Arrow), marked infiltration of lymphocytes and plasma cells.

while the left one was larger in two cases. The glands ranged in size from 24 to 35 mm in the maximum diameter on transverse images. None of the patients showed calcification or stones within the glands. The patients were divided into two groups according to the CT enhancement pattern: 11 cases showed rather homogeneous enhancement (**Figure 1A**); while in 9 cases the internal texture was characterized by multiple hyper-enhancing foci, demarcated with hypo-enhancing lines (**Figure 2A**), creating a crazy paving pattern (resembling paths made with pieces of stone or concrete). CT revealed prominent intraglandular vascularity in three patients, without significant mass effect. The maximum diameter of submandibular glands on transverse images in group 2 (3.2±0.4 cm) with crazy paving appearance was significantly larger than in group 1 with homogeneous enhancement (2.8±0.3 cm) according to Fisher's exact test (P=0.008).

Among the 20 patients, 16 showed enlargement of parotid glands, 5 of which were asymmetrical, with the right parotid gland larger than the left one. An abnormal density inside the parotid gland was present in 18 patients: there were 13 cases of multiple small nodules, with or without patchy or/and stripe-like lesions; 2 cases of multiple stripe-like lesions; and 3 cases of diffuse hyperdensity. Cervical lymphadenopathy was present in 10 patients. The density of the cervical lymph nodes was homogeneous both on the plain and contrast-enhanced images.

On histology, the normal submandibular gland structure was replaced by severe inflammatory cell infiltration and fibrosis in all patients. The interstitium was infiltrated by plasma cells and lymphocytes. Immunohistochemistry demonstrated that more than 40% of the plasma cells were IgG4+.

Direct comparison of CT and histological findings revealed that presence of thick fibrous bands correlated to hypo-enhancing lines in group 2 (**Figure 2**). The patients with thick fibrous bands on histology had crazy-paving pattern on CT, while those without the bands had homogenous enhancement (**Figure 1**).

Twelve patients had other IgG4-related conditions during the follow-up (3 months to 4 years), including lacrimal gland, parotid gland, pancreas, kidney, and lung involvement, as well as mediastinal and abdominal lymphadenopathy.

Discussion

The present study analyzed CT findings and pathologic characteristics in 20 patients with IgG4-RSD in the submandibular gland, which is the largest series of IgG4-RSD of the submandibular gland to date.

The salivary glands are the most frequently involved organs in IgG4-RSD of the head and neck [11], and the submandibular gland is the most frequently affected salivary gland [12]. Serum IgG4-levels can be helpful, but may be within or slightly above the normal range in many IgG4-related disease patients [4]. Additionally, IgG4 serum testing is not performed unless IgG4-RSD is considered clinically, and only a quarter of patients had serum IgG4-levels before surgery in our study.

The imaging features of IgG4-RSD in our series were not consistent with those described in previous reports, in which the salivary glands usually demonstrated homogeneous attenuation/signal intensity on CT/MR imaging, and homogeneous contrast enhancement [8-11]. In our study, the contrast-enhanced CT revealed the crazy-paving pattern in 9 cases. The histopathologic examination of the swollen submandibular glands revealed sclerosis of interlobular septa (fibrous bands) with resulting accentuation of the gland lobular architecture and an interstitial infiltrate of lymphocytes and plasma cells, which corresponded to CT findings. This suggests that the degree of sclerosis strongly influences the CT appearance.

In the study of Asai et al. [13], sonographic examination in 2 patients with IgG4-RSD revealed the internal texture of submandibular glands that had an appearance of multiple hypoechoic foci in rather hyperechoic parenchyma. However, CT and MRI showed only homogeneous submandibular glands. The authors concluded that CT and MRI cannot depict the details of the parenchymal change of the submandibular glands. In our study, the submandibular gland size in group 2 (with crazy-paving appearance) was significantly larger than in group 1 (with homogeneous enhancement). This may suggest that the crazy-paving pattern is becoming more frequent/conspicuous as the gland enlarges.

IgG4-RSD is a multisystemic disease that can involve many organs [1, 2]. Multiorgan disease may be evident at diagnosis but can also evolve metachronously, over months to years. For patients with AIP, additional examination reveals that 30% also have tubulointerstitial nephritis, indicated by radiologic findings and the presence of proteinuria and non-glomerular hematuria [14-18]. Recognition of IgG4-RSD in the submandibular glands is important as these patients may develop IgG4-related lesions in other sites. In our study, 12 patients had other IgG4-related involvement by systemic survey during follow-up. We propose that if CT findings suggest IgG4-RSD involvement in a patient with swollen submandibular glands, measurement of the serum IgG4 level as well as a systemic survey to search for related lesions in other organs should be considered. Characteristic imaging findings may also be diagnostic, avoiding unnecessary surgery.

The differential diagnosis of salivary gland IgG4-RSD includes malignant lymphoma. The CT appearance of lymphoma depends on the pathologic distribution of the disease. If the glandular parenchyma is involved, diffuse infiltration can be seen, exhibiting poorly defined margins or involving the entire gland. And the involvement is not restricted to the submandibular glands [19].

Several limitations of this study must be considered. First is the retrospective nature of the study with a relatively small number of patients. Second, CT was the only imaging modality. Further studies comparing different imaging modalities would be needed to determine the imaging characteristics as well as sensitivity and accuracy of each method for the parenchymal change of the submandibular glands with IgG4-RSD.

In summary, the submandibular glands with IgG4-RSD can be characterized by either homogeneous enhancement or crazy-paving pattern on contrast-enhanced CT imaging. It is important to increase awareness of IgG4-RSD, so that appropriate diagnostic evaluation can be performed to avoid unnecessary surgery.

Disclosure of conflict of interest

None.

Address correspondence to: Dr. Zhuhua Zhang, Department of Radiology, Peking Union Medical College Hospital, Shuaifuyuan 1#, Dongcheng District, Beijing 100730, China. Tel: 8610-69159544; 8610-15010147685; Fax: 8610-69155441; E-mail: pumchzhangyuhua@sina.com

References

[1] Stone JH, Zen Y and Deshpande V. IgG4-related disease. N Engl J Med 2012; 366: 539-551.

[2] Divatia M, Kim SA and Ro JY. IgG4-related sclerosing disease, an emerging entity: a review of a multi-system disease. Yonsei Med J 2012; 53: 15-34.

[3] Masaki Y, Dong L, Kurose N, Kitagawa K, Morikawa Y, Yamamoto M, Takahashi H, Shinomura Y, Imai K, Saeki T, Azumi A, Nakada S, Sugiyama E, Matsui S, Origuchi T, Nishiyama S, Nishimori I, Nojima T, Yamada K, Kawano M, Zen Y, Kaneko M, Miyazaki K, Tsubota K, Eguchi K, Tomoda K, Sawaki T, Kawanami T, Tanaka M, Fukushima T, Sugai S and Umehara H. Proposal for a new clinical entity, IgG4-positive mul-

tiorgan lymphoproliferative syndrome: analysis of 64 cases of IgG4-related disorders. Ann Rheum Dis 2009; 68: 1310-1315.
[4] Zen Y and Nakanuma Y. IgG4-related disease: a cross-sectional study of 114 cases. Am J Surg Pathol 2010; 34: 1812-1819.
[5] Bhatti RM and Stelow EB. IgG4-related disease of the head and neck. Adv Anat Pathol 2013; 20: 10-16.
[6] Hedgire SS, McDermott S, Borczuk D, Elmi A, Saini S and Harisinghani MG. The spectrum of IgG4-related disease in the abdomen and pelvis. AJR Am J Roentgenol 2013; 201: 14-22.
[7] Inoue D, Zen Y, Abo H, Gabata T, Demachi H, Kobayashi T, Yoshikawa J, Miyayama S, Yasui M, Nakanuma Y and Matsui O. Immunoglobulin G4-related lung disease: CT findings with pathologic correlations. Radiology 2009; 251: 260-270.
[8] Toyoda K, Oba H, Kutomi K, Furui S, Oohara A, Mori H, Sakurai K, Tsuchiya K, Kan S and Numaguchi Y. MR Imaging of IgG4-Related Disease in the Head and Neck and Brain. AJNR Am J Neuroradiol 2012; 33: 2136-2139.
[9] Katsura M, Mori H, Kunimatsu A, Sasaki H, Abe O, Machida T and Ohtomo K. Radiological features of IgG4-related disease in the head, neck, and brain. Neuroradiology 2012; 54: 873-882.
[10] Fujita A, Sakai O, Chapman MN and Sugimoto H. IgG4-related disease of the head and neck: CT and MR imaging manifestations. Radiographics 2012; 32: 1945-1958.
[11] Abe T, Sato T, Tomaru Y, Sakata Y, Kokabu S, Hori N, Kobayashi A and Yoda T. Immunoglobulin G4-related sclerosing sialadenitis: report of two cases and review of the literature. Oral Surg Oral Med Oral Pathol Oral Radiol Endod 2009; 108: 544-50.
[12] Ishida M, Hotta M, Kushima R, Shibayama M, Shimizu T and Okabe H. Multiple IgG4-related sclerosing lesions in the maxillary sinus, parotid gland and nasal septum. Pathol Int 2009; 59: 670-675.
[13] Asai S, Okami K, Nakamura N, Shiraishi S, Yamashita T, Anar D, Matsushita H and Miyachi H. Sonographic appearance of the submandibular glands in patients with immunoglobulin G4-related disease. J Ultrasound Med 2012; 31: 489-493.
[14] Raissian Y, Nasr SH, Larsen CP, Colvin RB, Smyrk TC, Takahashi N, Bhalodia A, Sohani AR, Zhang L, Chari S, Sethi S, Fidler ME and Cornell LD. Diagnosis of IgG4-related tubulointerstitial nephritis. J Am Soc Nephrol 2011; 22: 1343-1352.
[15] Yamamoto M, Harada S, Ohara M, Suzuki C, Naishiro Y, Yamamoto H, Takahashi H and Imai K. Clinical and pathological differences between Mikulicz's disease and Sjögren's syndrome. Rheumatology (Oxford) 2005; 44: 227-234.
[16] Sah RP, Pannala R, Chari ST, Sugumar A, Clain JE, Levy MJ, Pearson RK, Smyrk TC, Petersen BT, Topazian MD, Takahashi N and Vege SS. Prevalence, diagnosis, and profile of autoimmune pancreatitis presenting with features of acute or chronic pancreatitis. Clin Gastroenterol Hepatol 2010; 8: 91-96.
[17] Shimosegawa T and Kanno A. Autoimmune pancreatitis in Japan: overview and perspective. J Gastroenterol 2009; 44: 503-517.
[18] Tsubata Y, Akiyama F, Oya T, Ajiro J, Saeki T, Nishi S and Narita I. IgG4-related chronic tubulointerstitial nephritis without autoimmune pancreatitis and the time course of renal function. Intern Med 2010; 49: 1593-1598.
[19] Kato H, Kanematsu M, Goto H, Mizuta K, Aoki M, Kuze B and Hirose Y. Mucosa-associated lymphoid tissue lymphoma of the salivary glands: MR imaging findings including diffusion-weighted imaging. Eur J Radiol 2012; 81: e612-617.